J Physiol 590.14 (2012) pp 3231–3243

The Journal of Physiology

K^+–Cl^- cotransport mediates the bactericidal activity of neutrophils by regulating NADPH oxidase activation

Yuan-Ting Sun[1,2,3], Chi-Chang Shieh[1], Eric Delpire[4] and Meng-Ru Shen[5,6,7,8]

[1]*Institute of Clinical Medicine,* [2]*Department of Neurology,* [5]*Department of Pharmacology,* [6]*Department of Obstetrics & Gynecology,* [7]*Advanced Optoelectronic Technology Centre, and* [8]*Infectious Disease and Signaling Research Center, National Cheng Kung University Hospital, College of Medicine, National Cheng Kung University, Tainan 704, Taiwan*

[3]*Department of Internal Medicine, National Cheng Kung University Hospital, Dou-Liou Branch, Yun-Lin 640, Taiwan*

[4]*Department of Anaesthesiology, Vanderbilt University Medical Centre, Nashville, TN 37232, USA*

Key points

- Neutrophilic phagocytosis is essential for innate immunity against the bacterial infection.
- During phagocytosis, the generation of bactericidal hypochlorous acid requires superoxide produced by nicotinamide adenine dinucleotide phosphate (NADPH) oxidase to kill the internalized pathogens.
- We show that NADPH oxidase complexes are associated with K^+–Cl^- cotransporter (KCC) at the plasma membrane of activated neutrophils and are internalized to form phagosomes, where KCC activity and expression level affect the production of oxidants.
- This study supports the notion that KCC, in particular KCC3, is involved in the early stages of the host's defence against microorganisms.

Abstract Neutrophilic phagocytosis is an essential component of innate immunity. During phagocytosis, the generation of bactericidal hypochlorous acid (HOCl) requires the substrates, Cl^- and superoxide produced by nicotinamide adenine dinucleotide phosphate (NADPH) oxidase to kill the internalized pathogens. Here we show that the neutrophilic K^+–Cl^- cotransporter (KCC) constitutes a Cl^- permeation pathway and mediates the bactericidal activity by regulating NADPH oxidase activation. Dihydroindenyloxy alkanoic acid (DIOA), a KCC inhibitor, suppressed the toxin- or chemical-induced efflux of $^{36}Cl^-$ or $^{86}Rb^+$, and diminished the production of superoxide in human and murine neutrophils. Inhibition of KCC activity or knockdown of KCC expression, in particular KCC3, reduced the phosphorylation as well as the membrane recruitment of oxidase components. Activated neutrophils displayed a significant colocalization of KCC3 and early endosomal marker, indicating that KCC3 could be localized on the phagosomes once neutrophils are activated. The NADPH oxidase activity and the phosphorylation level of oxidase component were 50% lower in the neutrophils isolated from *KCC3*$^{-/-}$ mice than in the neutrophils isolated from *KCC3*$^{+/+}$ mice. Mortality rate after intraperitoneal challenge with *Staphylococcus aureus* was higher in *KCC3*$^{-/-}$ mice, and the bacterial clearance was impaired in the survivors. We conclude that, in activated neutrophil, NADPH oxidase complexes are associated with KCC3 at the plasma membrane and are internalized to form phagosomes, where KCC activity and expression level affect the production of oxidants.

(Received 29 November 2011; accepted after revision 16 April 2012; first published online 23 April 2012)

Corresponding author M.-R. Shen: Department of Obstetrics & Gynecology, National Cheng Kung University Hospital, Tainan 704, Taiwan. Email: mrshen@mail.ncku.edu.tw

DOI: 10.1113/jphysiol.2011.225300

Abbreviations CCC, cation–chloride cotransporter; CFTR, cystic fibrosis transmembrane conductance regulator; ClC, Cl^- channel; DIOA, dihydroindenyloxy alkanoic acid; fMLP, *N*-formyl-methionyl-leucyl-phenylalanine; KCC, K^+–Cl^- cotransporter; LPS, lipopolysaccharide; MPO, myeloperoxidase; NADPH, nicotinamide adenine dinucleotide phosphate; NCC, Na^+–Cl^- cotransporter; NKCC, Na^+–K^+–$2Cl^-$ cotransporter; PCR, polymerase chain reaction; PMA, phorbol 12-myristate 13-acetate; PMN, polymorphonuclear neutrophil; ROS, reactive oxygen species.

Introduction

Innate immunity is the first line of defence against infection. Polymorphonuclear neutrophils (PMNs) are essential for innate immunity against microorganisms. Neutrophils internalize and kill microbes by confining them within phagosomes containing reactive oxygen species (ROS) and hydrolytic enzymes. In the resting state, neutrophils are found with unusually high (80–100 mM) intracellular Cl^- concentrations ($[Cl^-]_i$), which are 4- to 5-fold higher than what is predicted on the basis of the Nernst equation (Simchowitz & De Weer, 1986; Ince *et al.* 1987). This high internal Cl^- seems to be essential for Cl^- efflux during neutrophil activation. Several pieces of evidence have pointed out the importance of Cl^- in activated neutrophils. During the early phase of neutrophil activation, there is a β2 integrin-mediated adhesion-dependent clearance of $[Cl^-]_i$ (Menegazzi *et al.* 1996, 1999, 2000). At the late phase of activation, another significant and irreversible Cl^- efflux occurs during phagocytosis (Busetto *et al.* 2007), and the myeloperoxidase (MPO) produces hypochlorous acid (HOCl), a potent bactericidal chemical in innate immunity, from the substrates hydrogen peroxide (H_2O_2) and Cl^- (Allegra *et al.* 2001).

Previous studies have identified several Cl^- permeation pathways in activated neutrophils (Moreland *et al.* 2006, 2007; Graves *et al.* 2008; Painter *et al.* 2008; Salmon & Ahluwalia, 2009; Bonvillain *et al.* 2010; Matsuda *et al.* 2010). For example (1) ClC-3 is involved in the regulation of phagocyte nicotinamide adenine dinucleotide phosphate (NADPH) oxidase activity following chemotactic stimulation or endotoxin priming (Moreland *et al.* 2006, 2007; Matsuda *et al.* 2010); (2) the cystic fibrosis transmembrane conductance regulator (CFTR) contributes the biosynthesis of HOCl and bactericidal activity (Painter *et al.* 2008; Bonvillain *et al.* 2010); and (3) the swelling-activated chloride channel (ICl_{swell}), which is activated by hypotonic shock, counteracts the membrane depolarization that resulted from the activation of NADPH oxidase (Salmon & Ahluwalia, 2009). The participation of Cl^- permeation pathways in respiratory burst highlights the crucial role of Cl^- in innate immunity.

Considering the Cl^- permeation and cell volume sensitive properties in the above-mentioned literatures, here we study the unaddressed function of K^+–Cl^- cotransporter (KCC) in innate immunity. KCC is a member of CCC family, which also includes the Na^+–K^+–$2Cl^-$ cotransporter (NKCC) and the Na^+–Cl^- cotransporter (NCC). It mediates the coupled electroneutral movement of K^+ and Cl^- across the plasma membrane with concurrent water flux in response to cell swelling and plays an important role in ionic homeostasis, cell morphology, cell division and cell migration (Adragna *et al.* 2004). Through pharmacological approaches, RNAi knockdown techniques, and a genetic knockout animal model, we show that NADPH oxidase complexes are associated with KCC at the plasma membrane of activated neutrophils and are internalized to form phagosomes, where KCC activity and expression level affect the production of oxidants. KCC also might be one of the Cl^- permeation pathways providing the substrate for the generation of bactericidal hypochlorous acid in phagosomes.

Methods

Ethical approval

The animal study was carried out in strict accordance with the recommendations in the *Guide for the Care and Use of Laboratory Animals* of the National Institutes of Health. The protocol was approved by the Institutional Animal Care and Use Committee (IACUC) of National Cheng Kung University (IACUC Approval No. 98178). Surgery was performed under sodium pentobarbital anaesthesia (40 mg kg^{-1}) and all efforts were made to minimize suffering. All clinical investigations were conducted according to the principles expressed in the Nuremberg Code and *Declaration of Helsinki*. The protocol of human subjects was approved by the Institutional Review Board of National Cheng Kung University Hospital (IRB Approval No. ER-99-212). Human subjects involved had the legal capacity to give voluntary consent. Physicians had endeavored to disclose the research-relevant information to the subjects. Subjects who agreed to participate signed an Informed Consent Form acknowledging that agreement.

Preparation of human and murine PMNs

Human PMNs from healthy consenting adults (16 subjects, 4 males and 12 females, 25–44 years old) were obtained by Ficoll-Hypaque gradient centrifugation (English and Andersen, 1974). Purified PMNs were resuspended in 1× Hanks' balanced salt solution (HBSS), without calcium or magnesium, and then washed. Murine

PMNs were isolated from blood collected by cardiac puncture. Procedures for density centrifugation were the same as described above.

Cell culture and differentiation

The human myeloid cell line HL-60 was grown in RPMI-1640 medium (Caisson Laboratories, North Logan, UT, USA) containing 10% fetal bovine serum (FBS; BD Biosciences), 100 U ml^{-1} penicillin, and 100 $\mu g\ ml^{-1}$ streptomycin (Sigma-Aldrich, St Louis, MO, USA) at 37°C in a humidified 5% CO_2 atmosphere. For granulocyte differentiation, HL-60 cells were incubated in culture medium supplemented with dimethyl sulfoxide (DMSO, 0.3 μM/0.3%) for 72 h. Induction of differentiation was performed 7 days prior to all experiments. Human embryonic kidney cells (HEK-293T) were grown in Dulbecco's modified Eagle's medium supplemented with 10% FBS, penicillin and streptomycin.

RNA interference with shRNA

The target sequences for three KCC isoforms are listed in Table S1. The oligonucleotides conjugated to sites on the lentiviral vector of pLKO.1 (which carries a puromycin-resistance gene) were obtained from National RNAi Core Facility at Academia Sinica, Taipei, Taiwan. The vector plasmids, together with the gag-pol plasmid (pCMV ΔR8.91) and the VSV-G envelope encoding plasmid (pMD.G) were amplified in bacteria, purified using the Maxiprep Kit (Qiagen, Hilden, Germany), and mixed with $CaCl_2$ (Sigma-Aldrich), then with 2× Hepes (Sigma-Aldrich) and added to 80% confluent HEK-293T cells (Liu *et al.* 2011). After 48 h, the supernatant was collected and centrifuged. The lentivirus was titrated using HEK-293T cells. The number of infectious virus particles per microlitre was estimated by determining the percentage of cells resistant to puromycin from the linear portion of the curve 48 h later. Lentivirus-mediated small hairpin RNA against KCC1 (shKCC1), KCC3 (shKCC3), KCC4 (shKCC4) and luciferase (as a vector control) were delivered into undifferentiated HL-60 cells ($10^5\ ml^{-1}$) with multiplicity of infection (MOI) = 4 for 24 h, followed by puromycin (4 $\mu g\ ml^{-1}$) selection for 72 h. The live HL-60 cells were separated from the dead cells by gradient centrifugation using Ficoll Paque Plus reagent (GE Healthcare, Piscataway, NJ, USA). Quantitative RT-PCR and immunoblotting were performed to validate the knockdown efficiency. Granulocyte differentiation was induced in KCC knocked down HL-60 cells prior to experiments.

Semi-quantitative and quantitative reverse transcription-PCR

For reverse-transcription polymerase chain reaction (PCR), total RNA was extracted using an RNeasy Mini Kit (Qiagen, Hamburg, Germany) according to the manufacturer's instructions. Reverse transcription was performed using total RNA, random hexamers as primers, dNTPs (dinucleotide triphosphates), dithiothreitol, and Superscript II reverse transcriptase (Invitrogen). Semi-quantitative PCRs were done with the primers listed in Table S1. The PCR reactions yielded 421 bp, 1099 bp and 783 bp fragments for KCC1, KCC3 and KCC4, respectively. Quantitative PCRs were done with the primers and probes listed in Table S1.

KCC3 knockout animals

KCC3$^{-/-}$ mice were generated through homologous recombination as previously described (Sun *et al.* 2010). Genotyping was performed through separate PCRs with 1 μl of tail DNA to amplify fragments specific to KCC3 control and mutant genes using the following primers: control gene forward 5′-GAACTTTGTGTTGATTCCTTTGG-3′ and reverse 5′-TCTCCTAACTCCATCTCCAGGG-3′ primers; mutant gene forward 5′-GAACTTTGTGTTGATTCCTTTGG-3′ and reverse 5′-TACAACACACACTCCAACCTCCG-3′ primers. The PCR reactions yielded 371 bp and 290 bp fragments for the control and mutant, respectively.

PMN stimulation

Differentiated HL-60 cells, human or murine PMNs were pre-incubated with 50 μM dihydroindenyloxy alkanoic acid (DIOA; Alexis Biochemicals, San Diego, CA, USA), 20 μM bumetanide (Sigma-Aldrich), or 0.1% DMSO at 37°C for 45 min. Afterward, phorbol 12-myristate 13-acetate (PMA; Sigma-Aldrich), *N*-formyl-methionyl-leucyl-phenylalanine (fMLP; Sigma-Aldrich), or lipopolysaccharide (LPS; *E. coli* serotype 0111:B4; Sigma-Aldrich) was then added to a final concentration of 10 nM, 20 μM, or 0.4 $\mu g\ ml^{-1}$, respectively. For PMA or fMLP stimulation, cells were incubated with PMA or fMLP for 10 min and then collected for ROS detection, immunoblotting, immunofluorescence study or flux experiments. For PMN priming by LPS, cells were initially incubated with 0.4 $\mu g\ ml^{-1}$ LPS for 20 min and then another 0.4 $\mu g\ ml^{-1}$ LPS was added. Cells were futher incubated with LPS for another 10 min before the collection for studies.

Measurement of NADPH oxidase activity

Lucigenin-enhanced chemiluminescence assays for NADPH oxidase activity were performed by using the high-performance Chemiluminescence Analyser System (CLA-2100; Tohoku Electronic Inc., Sendai, Japan). A PMN suspension containing 2.5×10^6 PMNs ml^{-1} in HBSS was added to each well with a 100 μM final concentration of lucigenin (Sigma-Aldrich). Chemiluminescence was quantified as relative luminescence units using a kinetic assay with readings taken every minute.

$^{36}Cl^-$ or $^{86}Rb^+$ efflux assays

Efflux experiments were carried out according to the detailed protocol of our previous studies (Shen *et al.* 2001*a*,*b*). In brief, PMNs were preincubated with isotonic HBSS (without Ca^{2+} or Mg^{2+}), loaded with 2 μCi ml^{-1} $^{36}Cl^-$ or $^{86}Rb^+$ for 1 h at 37°C. Then appropriate efflux medium (containing 0.1 mM ouabain and 0.01 mM bumetanide to inhibit the Na^+–K^+ pump and NKCC activities, respectively) was added to the washed PMNs. Release of $^{36}Cl^-$ or $^{86}Rb^+$ from preloaded cells was measured from the efflux medium at indicated time intervals (1, 5, 10 or 20 min) within a 20 min duration. Efflux rate constant was estimated from the negative slope of the graph of $\ln[X_i\ (t)/X_i\ (t=0)]$ *vs.* time (t), where $X_i\ (t=0)$ denotes the total amount of $^{36}Cl^-$ or $^{86}Rb^+$ inside the cells at the beginning of the efflux time course and $X_i(t)$ denotes the amount of $^{36}Cl^-$ or $^{86}Rb^+$ inside the cells at the time point t ($t = 1$, 5, 10 or 20 min).

Immunoblotting and immunofluorescence

Equal amounts of denatured protein from lysed PMNs (40 μg in each lane) were separated on 12.5% polyacrylamide gels and transferred to Biotrace NT Nitrocellulose Transfer Membranes (Pall Life Science, Ann Arbor, MI, USA). The primary antibodies used were polyclonal anti-KCC1, -KCC3, -KCC4 (1:1000 for immunoblotting and 1:100 for immunofluorescence; Santa Cruz Biotechnology, Santa Cruz, CA, USA), polyclonal anti-phospho-p40^{phox} (1:1000; Cell Signaling Technology, Danvers, MA, USA) and monoclonal anti-β-actin (1:10,000; Sigma-Aldrich). The secondary antibodies were horseradish peroxidase-conjugated anti-mouse antibodies (1:20,000; BD Biosciences Pharmingen, San Jose, CA, USA) or anti-rabbit or anti-goat secondary antibodies (1:2000; BD Biosciences Pharmingen). For immunofluorescence staining, neutrophil suspensions were fixed in 3.7% paraformaldehyde in PBS and permeabilized with 0.1% Triton X-100. Primary antibodies used here were polyclonal rabbit anti-p40^{phox} (1:100, GeneTex, San Antonio, TX, USA), polyclonal rabbit anti-p47^{phox} (1:100, Santa Cruz Biotechnology), polyclonal goat anti-p67^{phox}, polyclonal rabbit anti-EEA1(1:100, Cell Signalling Technology), and the secondary antibodies were Alexa Fluor 488 and 594 (1:200, Invitrogen Life Technologies, Carlsbad, CA, USA). Cells after washing were mixed with gelatin, mounted and visualized in a confocal microscope. To quantify the ratio of membrane recruitment, the immunifluorescence intensities of phox proteins in membrane or juxtamembrane area (~1.5 μm beneath the membrane) were obtained and divided by the intensity of whole neutrophil. The colocalization ratio was determined by the analysis software of FV1000 (Olympus, Japan).

Infection experiments in mice

S. aureus (ATCC No. 25923) was grown overnight at 37°C in 5 ml of Luria–Bertani broth and subcultured into 50 ml of LB broth at a 1:50 dilution and grown for 6 h. *S. aureus* density was determined spectrophotometrically and confirmed by plating onto 5% Trypticase soy agar plates. Two-month-old *KCC3*$^{+/+}$ and *KCC3*$^{-/-}$ mice were injected intraperitoneally with *S. aureus* (2.36×10^8 colony forming units). The condition of the mice was monitored for 7 days. To determine the severity of the infection, surviving animals were killed 7 days after injection. The intra-abdominal condition was observed, and the intestinal lymph nodes were counted.

Histopathology

The isolated small intestines were fixed in 3.7% paraformaldehyde for 3–4 h, dehydrated in a graded series of ethanol solutions, treated with xylene, paraffin-embedded, and cut into 4 μm-thick longitudinal sections. Sections were deparaffinized in xylene and rehydrated in graded ethanol solutions for standard hematoxylin–eosin staining.

Statistical analysis

Values are given as means ± SEM. Data were compared using Student's t test, and differences were considered significant at $P < 0.05$. Kaplan–Meier survival analysis was applied to compare survival between the *KCC3*$^{+/+}$ and *KCC3*$^{-/-}$ mice. Differences were considered significant at $P < 0.05$.

Results

KCC activity is increased in activated PMNs

We first tested whether the KCC-mediated K^+ or Cl^- efflux is increased with PMN activation. As shown in Fig. 1*A* and *B*, $^{36}Cl^-$ efflux is markedly increased

in PMNs treated with endotoxin lipopolysaccharide (LPS) or phorbol 12-myristate 13-acetate (PMA). This efflux is dose-dependently inhibited by a KCC inhibitor, dihydroindenyloxy alkanoic acid (DIOA). In complementary K^+ transport experiments, both LPS- and PMA-induced ouabain- and bumetanide-insensitive K^+ efflux were completely abolished by 50 μM DIOA (Fig. 1*C* and *D*). DIOA itself did not affect the basal Cl^- and K^+ efflux in resting human neutrophils or the viability of neutrophils (Fig. S1). These results indicate that the KCC activity is increased with PMN activation. The molecular identification by RT-PCR and immunoblotting confirms the presence of the KCC family in human PMNs and the HL-60 cell line (Fig. S2).

KCC is involved in ROS generation

The role of KCC and NKCC (both are members of CCC family) in the activation of NADPH oxidase was assessed by chemiluminescence assay. PMA provoked a marked increase of ROS production lasting >30 min in human neutrophils (Fig. 2*A*). This effect was dose-dependently inhibited by DIOA. The half-maximal inhibitory concentration (IC_{50}) of DIOA for suppressing ROS generation determined from a dose–response curve was 16 μM (Fig. 2*B*), which is similar to the concentration of inhibiting KCC activity (Garay *et al.* 1988). In contrast, bumetanide, an NKCC inhibitor, showed no inhibitory effect on PMA-induced ROS generation (Fig. 2*B*). Similar results were obtained by using other chemotactic factors, such as fMLP and LPS (Fig. 2*C* and *D*). Moreover, the identical phenomena were found in murine PMNs as well as HL-60 cells (Fig. S3). These results indicate that KCC, but not NKCC, is involved in the ROS production of activated neutrophils.

KCC regulates the phagocytic NADPH oxidase

The NADPH oxidase is a membrane-bound enzyme complex made up of six subunits. These subunits are a Rho GTPase and five NOX2 components ($p22^{phox}$, $p40^{phox}$, $p47^{phox}$, $p67^{phox}$, and $gp91^{phox}$). Under normal circumstances, the complexes of NADPH oxidase are latent in neutrophil cytosol and are activated with phosphorylation to assemble in the membranes during respiratory burst. The phosphorylation levels of these phox components, in particular $p40^{phox}$, are correlated with the level of superoxide production (Fuchs *et al.*

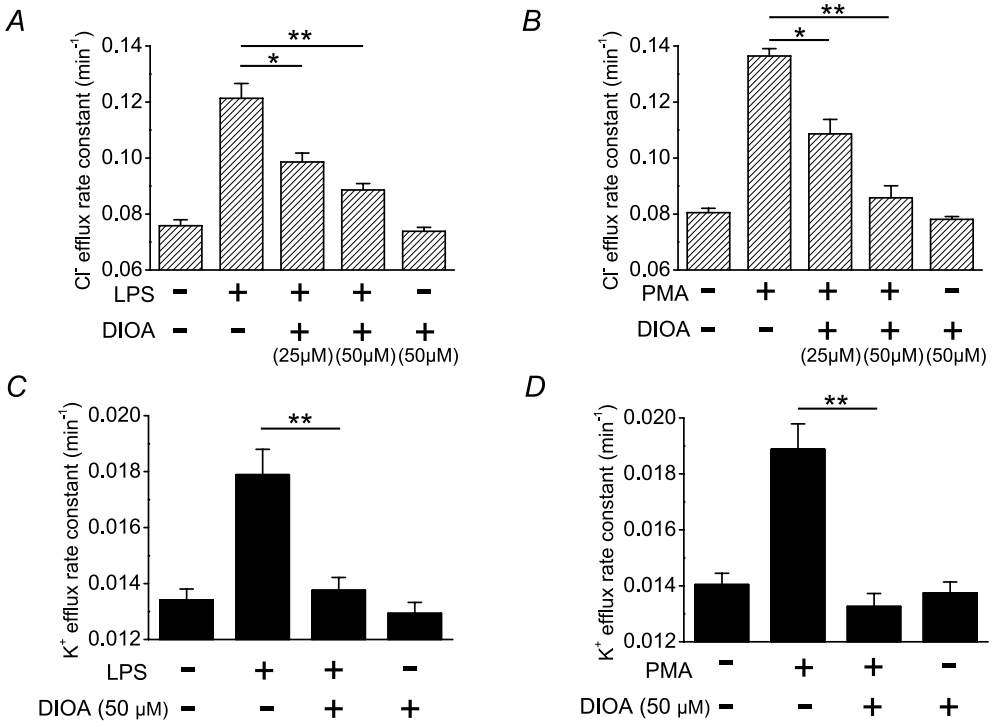

Figure 1. K^+ and Cl^- efflux in human neutrophils
LPS or PMA increased the Cl^- (*A* and *B*) and K^+ (*C* and *D*) efflux in human neutrophils. The increased K^+ or Cl^- efflux was significantly inhibited by DIOA, a KCC inhibitor. K^+ efflux was determined using $^{86}Rb^+$ as a congener. The medium for $^{36}Cl^-$ and $^{86}Rb^+$ efflux assays contained 0.1 mM ouabain and 0.01 mM bumetanide to inhibit the Na^+–K^+ pump and NKCC activities, respectively. The detailed protocols for neutrophil stimulation and flux measuarement were described in Methods. Each value represents the mean ± SEM ($n = 5$). *$P \leq 0.05$, **$P \leq 0.01$. DIOA, dihydroindenyloxy alkanoic acid; LPS, lipopolysaccharide; PMA, phorbol 12-myristate 13-acetate.

1997). To study the mechanisms of KCC in regulating ROS production, we examined the effect of KCC activity on membrane recruitment and phosphorylation of phox components. As shown in Fig. 3*A*, PMA remarkably increased the phosphorylation level of $p40^{phox}$, which was almost abolished by DIOA but not by bumetanide. DIOA or bumetanide itself did not alter the basal phosphorylation level of $p40^{phox}$. This implies that KCC activity, but not NKCC activity, is required for the phosphorylation of $p40^{phox}$. Phosphorylation induces conformational changes in phox proteins thereby bringing the phox units to the membrane, which is a signature event for NADPH oxidase activation (El-Benna *et al.* 2009). The membrane recruitment of $p40^{phox}$, $p47^{phox}$ and $p67^{phox}$ proteins upon neutrophil activation was further studied by immunofluorescence staining. In the representative micrographs showing in Fig. 3*B*, the control group displayed a diffuse cytosolic localization of $p47^{phox}$. With PMA stimulation, punctae of $p47^{phox}$ were formed at the membrane periphery. DIOA, but not bumetanide, reduced the PMA-provoked membrane recruitment of $p47^{phox}$ proteins. Neither DIOA nor bumetanide triggered the translocation of $p47^{phox}$. Other oxidase components such as $p40^{phox}$ and $p67^{phox}$ also remained diffusely distributed in cytoplasm during latency. In striking contrast, PMA induced the assembly of $p40^{phox}$ and $p67^{phox}$ into punctae that were recruited to the juxta-membrane region (Fig. 3*C*). In the quantitative analysis at the juxta-membrane region, the colocaliztion ratio of $p40^{phox}$ and $p67^{phox}$ significantly rises from less than 5% to 40%. DIOA diminished the complex formation of $p40^{phox}$ and $p67^{phox}$ in PMA-stimulated PMNs (Fig. 3*C*). Figure 3*D* summarized the quantitative analyses for the membrane recruitment of different phox units at various experimental conditions.

KCC3 knockdown inhibits NADPH oxidase activation

Our experiments using pharmacological inhibitors showed the importance of KCC activity in neutrophil activation. However, DIOA is not an isoform-specific KCC inhibitor. To exclude the off-target effect of DIOA and to weigh the contribution of individual KCC isoform, KCC1,

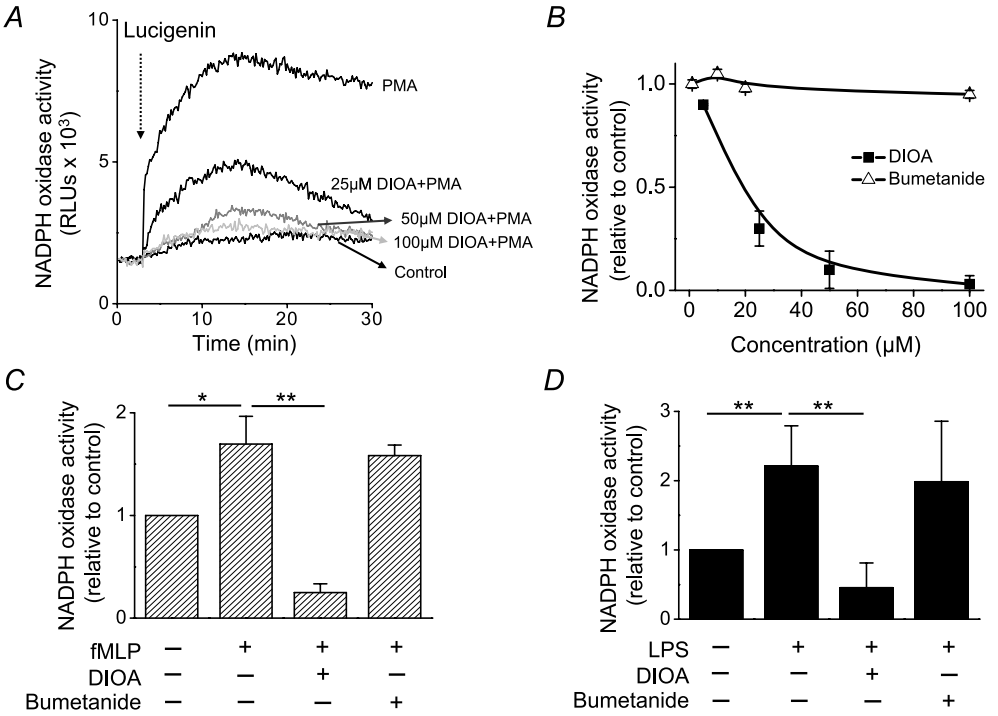

Figure 2. The KCC inhibitor, but not NKCC inhibitor, diminished the ROS production in human neutrophils

A, the representative real-time cumulated ROS recordings by the chemiluminescence assay. After pre-incubation with DIOA or 0.1% DMSO at 37°C for 45 min, human neutrophils were then stimulated by PMA (10 nM) for 10 min. Lucigenin (arrow) was injected to detect the NADPH oxidase activity in human neutrophils. The control group was neutrophils treated with 0.1% DMSO alone without PMA stimulation. *B*, dose–response curves showing the effect of DIOA or bumetanide on PMA-provoked ROS generation in human neutrophils. *C* and *D*, effect of DIOA (50 μM) or bumetanide (20 μM) on fMLP or LPS-stimulated ROS generation in human neutrophils. The control group was neutrophils treated with 0.1% DMSO alone without toxin stimulation. The ROS production in each experimental group was expressed relative to control group. Each value represents the mean ± SEM from at least five different samples. RLU, relative luminescence unit. $^{*}P \leq 0.05$; $^{**}P \leq 0.01$.

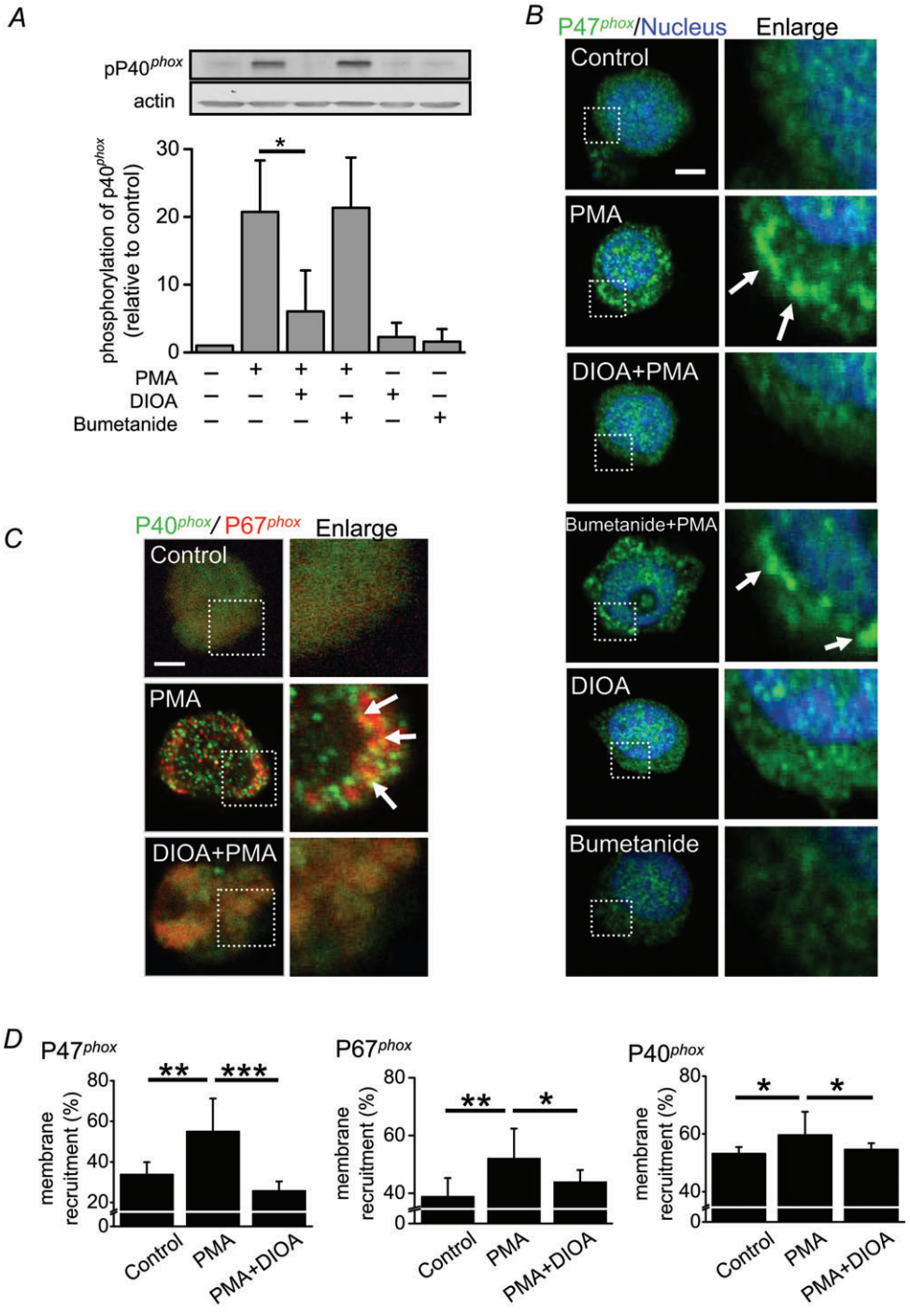

Figure 3. KCC activity regulated the NADPH oxidase of human neutrophil
A, the phosphorylation of phox units in human neutrophils. A representative immunoblot showed the phosphorylation levels of p40^{phox} in human neutrophils at various experimental conditions. The control group was neutrophils treated with 0.1% DMSO alone. The detailed protocols for neutrophil stimulation were described in Methods. *B* and *C*, PMA induced the membrane recruitments of phox units (p47^{phox}, p40^{phox} and p67^{phox}). PMA caused the puncta formation of p47^{phox}, especially at the membrane periphery (*B*). DIOA, but not bumetanide, reduced the PMA-provoked membrane recruitment of p47^{phox} proteins. Other oxidase components such as p40^{phox} and p67^{phox} also remained diffusely distributed in cytoplasm during latency. PMA induced the assembly of p40^{phox} and p67^{phox} into complexes that were recruited to the juxta-membrane region (*C*). *D*, the quantitative analyses for the membrane recruitment of different phox units at various experimental conditions. Each value represents the mean ± SEM from three different experiments by analysing at least 30 cells. $^*P \leq 0.05$, $^{**}P \leq 0.01$, $^{***}P \leq 0.005$. Scale bar, 2 μm.

KCC3 and KCC4 were knocked down individually in HL-60 cells. The knockdown efficiencies of three shKCC1, three shKCC3 and three shKCC4 oligonucleotides were tested (Fig. S4). The expression of the other two KCC isoforms apart from the targeted one was also assessed to rule out the possible compensatory expression. Eventually we chose shKCC1#5, shKCC3#6, and shKCC4#20 for further experiments. PMA stimulation in wild-type and vector-control (shLuciferase) cells provoked a marked increase of ROS generation, whereas PMA-induced ROS generation was reduced by 70–80% in shKCC3 cells (Fig. 4*A*). Silencing of KCC1 or KCC4 showed a mild to moderate inhibitory effect on NADPH oxidase activity. In addition, KCC3 knockdown almost abolished PMA-induced phosphorylation of $p40^{phox}$, whereas KCC1 or KCC4 knockdown showed about 50% reduction in the PMA-induced phosphorylation of $p40^{phox}$ compared to that of shLuciferase cells (Fig. 4*B*). The phosphorylation levels of $p40^{phox}$ in all shKCC cell lines were checked to exclude clonal effects (Fig. S5). PMA induced the phosphorylation of $p40^{phox}$ to different extents in wild-type, shLuciferase, shKCC1 and shKCC4 cell lines. In contrast, PMA did not induce a significant phosphorylation of $p40^{phox}$ in three shKCC3 HL-60 cell lines. The membrane recruitment of $p47^{phox}$ was also markedly diminished in shKCC3 cells in response to PMA stimulation (Fig. 4*C*). NADPH oxidase activity and the regulation of oxidase components were similar between

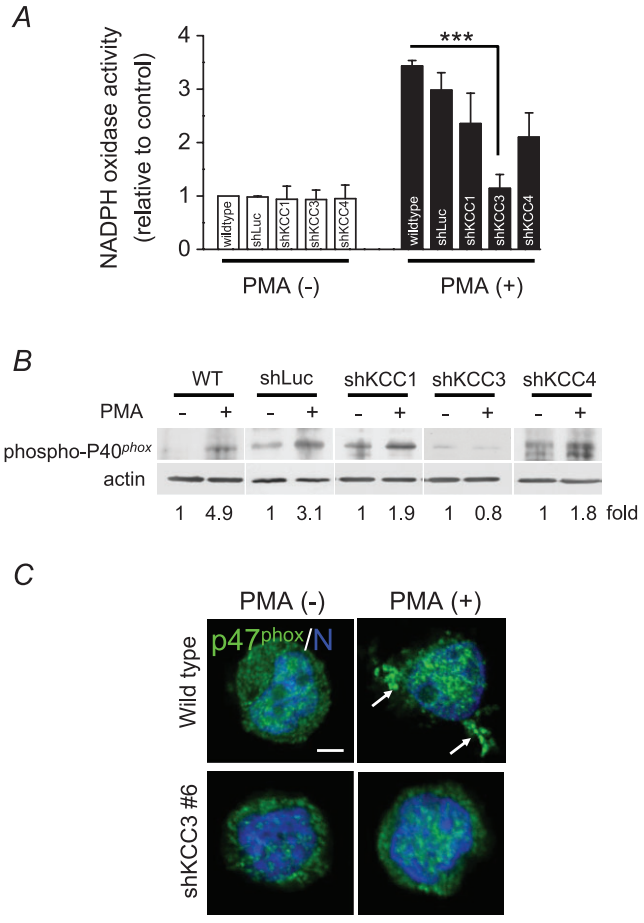

Figure 4. KCC3 knockdown inhibited NADPH oxidase activation in HL-60 cells
A, NADPH oxidase activity as indicated by ROS generation in wild-type, shLuciferase (shLuc) shKCC1, shKCC3 and shKCC4 HL-60 cells. The ROS production in wild-type HL-60 cells without PMA stimulation was used as the control and the others were expressed relative to the control. *B*, a representative immunoblot of phosphorylated $p40^{phox}$ in wild-type, shLuciferase (shLuc), shKCC1, shKCC3 and shKCC4 HL-60 cells from three independent experiments. *C*, the membrane recruitment of $p47^{phox}$ was significantly diminished in shKCC3 cells in response to PMA stimulation. Representative images were from three different experiments. $^{***}P \leq 0.005$; scale bar: 2 μm; N: nucleus; arrow: membrane recruitment of $p47^{phox}$.

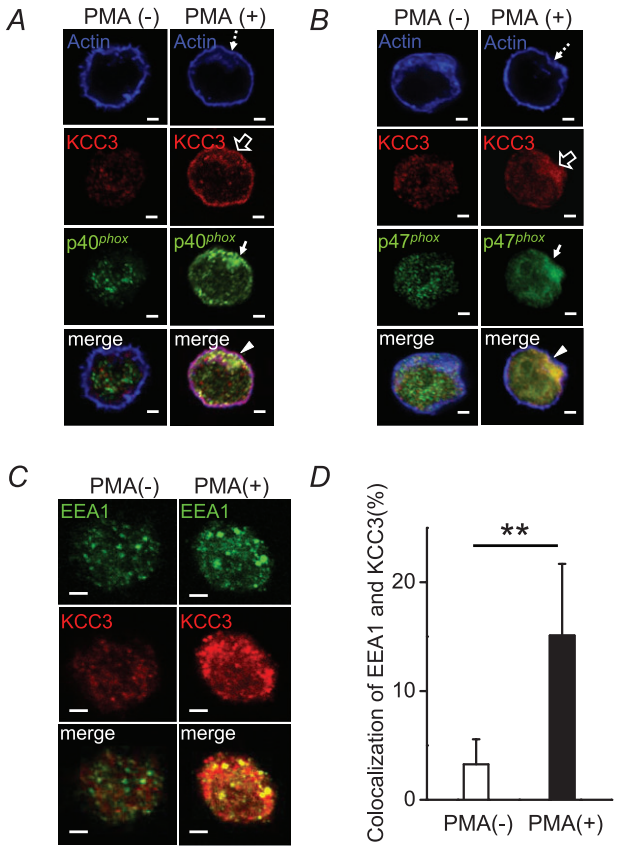

Figure 5. The distribution of KCC3, NADPH oxidase and phagosomes in human neutrophils
A and *B*, with PMA stimulation, KCC3, $p40^{phox}$ and $p47^{phox}$ were recruited to the juxta-membrane area, where KCC3, phox units and actin formed a complex. *C*, KCC3 could be re-located to phagosomes in activated neutrophils. In resting neutrophils, very few KCC3 and EEA1 (an early endosomal marker) were localized together. Activated neutrophils displayed a significant colocalization of KCC3 and EEA1. *D*, the quantitative analyses for the colocaliztion of KCC3 and EEA1. Each value represented the mean ± SEM from three independent experiments by analysing at least 25 cells. $^{**}P \leq 0.01$; scale bar: 2 μm.

shLuciferase and wild-type cell lines (Fig. S6). These results highlight the important role of KCC3 in the regulation of NADPH oxidase activation.

KCC3 could be re-located to phagosomes in activated neutrophils

Since KCC3 and phox components are all membrane proteins, we studied their possible direct association. As shown in Fig 5*A* and *B*, PMA induced the membrane recruitment of phox components that were colocalized with KCC3. These results raise the possibility that KCC3 initially is localized on the cell membrane and then re-locates to phagosomes, or that stimulation causes NADPH oxidase complex to associate with KCC3 at the plasma membrane and then subsequently forms a phagosome. To study the possibility of KCC3 relocalization, neutrophils were double-stained with KCC3 and EEA1, an early endosomal marker (Fig. 5*C*). In resting neutrophils, very few KCC3 and EEA1 were localized together (Fig. 5*C*). In striking contrast, activated neutrophils displayed a significant colocalization of KCC3 and EEA1 (Fig. 5*C* and *D*). These data imply that KCC3 could be localized on the phagosomes once neutrophils are activated.

KCC3-deficient neutrophils manifest a reduced NADPH oxidase activity

Since KCC3 plays an important role in NADPH oxidase activation, KCC3 knockout might show an impaired immunity. We therefore utilized KCC3-deficient mice to test this hypothesis. $KCC3^{-/-}$ and $KCC3^{+/+}$ PMNs show a similar basal NADPH activity (Fig. 6*A* and *B*). With PMA stimulation, $KCC3^{-/-}$ PMNs displayed a significantly weaker response of ROS production, compared to that of $KCC3^{+/+}$ murine PMNs (Fig. 6*B*, $P < 0.01$). In addition, $KCC3^{-/-}$ neutrophils exhibited a 50% reduction in PMA-induced $p40^{phox}$ phosphorylation, as compared to $KCC3^{+/+}$ PMNs ($P < 0.05$, Fig. 6*C*). The significant reduction in the NADPH oxidase activity of $KCC3^{-/-}$ PMNs was consistent with the findings of pharmacological experiments and RNAi knockdown experiments (Figs 2–5). These results confirm the important role of KCC3 in the regulation of ROS production. The blood profiles of wild-type and $KCC3^{-/-}$

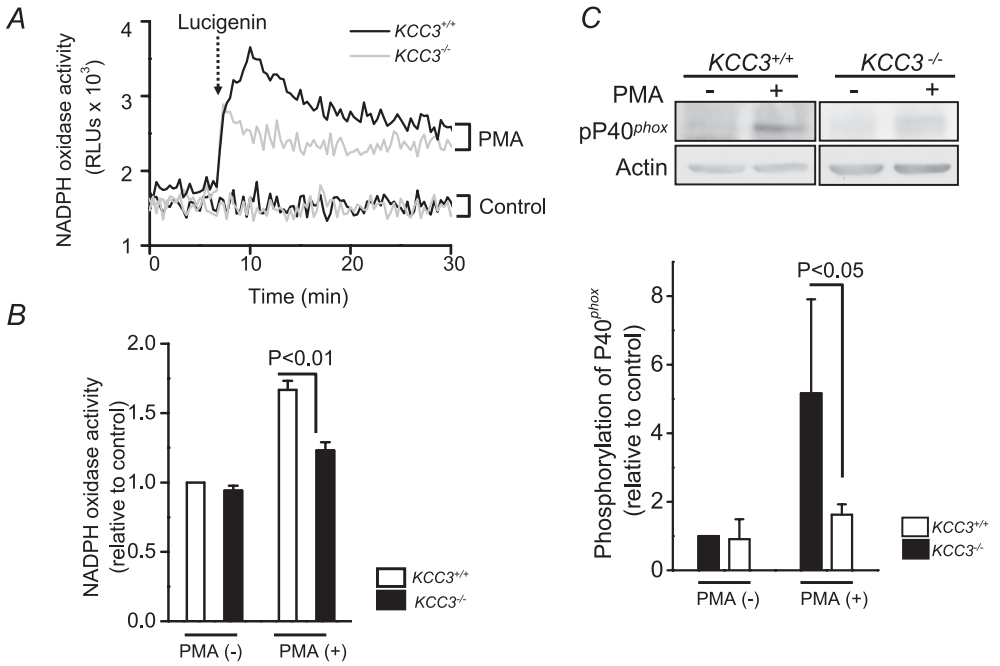

Figure 6. NADPH oxidase activity in $KCC3^{+/+}$ and $KCC3^{-/-}$ murine neutrophils
A, the representative real-time cumulated ROS recordings by the chemiluminescence assay in $KCC3^{+/+}$ and $KCC3^{-/-}$ murine neutrophils with or without 10 nM PMA stimulation. The dotted arrow indicated the adding of lucigenin. The control group was neutrophils treated with 0.1% DMSO alone. *B*, impaired ROS production in $KCC3^{-/-}$ murine neutrophils. The area under the curve was calculated as the total ROS production for a 30 min period after adding lucigenin. The ROS production in $KCC3^{+/+}$ group without PMA stimulation was used as the control and the others were expressed relative to the control. Each value represented the mean ± SEM ($n = 6$). *C*, a representative immunoblot of phosphorylated $p40^{phox}$ in $KCC3^{+/+}$ and $KCC3^{-/-}$ neutrophils from three independent experiments. The phosphorylation level of $p40^{phox}$ in the $KCC3^{+/+}$ group without PMA stimulation was used as the control and the others were expressed relative to the control.

mice are listed in Table S2. Except for white blood cell counts, haematological indices were essentially equivalent and similar to those previously reported (Rust *et al.* 2007). $KCC3^{-/-}$ mice showed an increased white blood cell count ($P < 0.05$) and an elevated neutrophil/lymphocyte ratio, which is likely to be a compensation for dysfunctional neutrophils.

KCC3-deficient mice are more susceptible to infectious challenge

To determine whether the insufficient KCC activity impairs the host defence against bacteria, we subjected $KCC3^{-/-}$ and wild-type littermates to intraperitoneal injection of *Staphylococcus aureus*. Among nine $KCC3^{-/-}$ mice in the experiments, three died within 4 days of intraperitoneal infection, whereas all wild-type animals survived beyond the 7 day duration of the experiments. Wild-type mice had a significant survival advantage over $KCC3^{-/-}$ mice during the 7 day period (Fig. 7*A*, $P < 0.05$). To compare the severity of the pyogenic infection in surviving $KCC3^{-/-}$ and wild-type mice, the appearance of the intra-abdominal region was assessed (Fig. 7*B* and *C*). $KCC3^{-/-}$ mice showed various typical signs of ileus and peritonitis: intestinal distention with stool impaction (78%), hyperaemic peritoneum (55%), pus formation (55%), and white caseous colonies in the peritoneum, liver surface, or omentum (33%). In contrast, most of $KCC3^{+/+}$ mice (80%) showed no intra-abdominal signs of infection (Fig. 7*C*). Enlarged intestinal lymph nodes were noted in all surviving $KCC3^{-/-}$ mice and in some wild-type mice, but their number was significantly lower in wild-type mice than in $KCC3^{-/-}$ mice (Fig. 7*D* and *E*). Lymphoid protrusions dissected from $KCC3^{-/-}$ mice consisted of prominent germinal centres containing abundant apoptotic bodies (Fig. 7*F*). The higher mortality and greater severity of intra-abdominal inflammation suggest the impaired bacterial clearance in $KCC3^{-/-}$ mice.

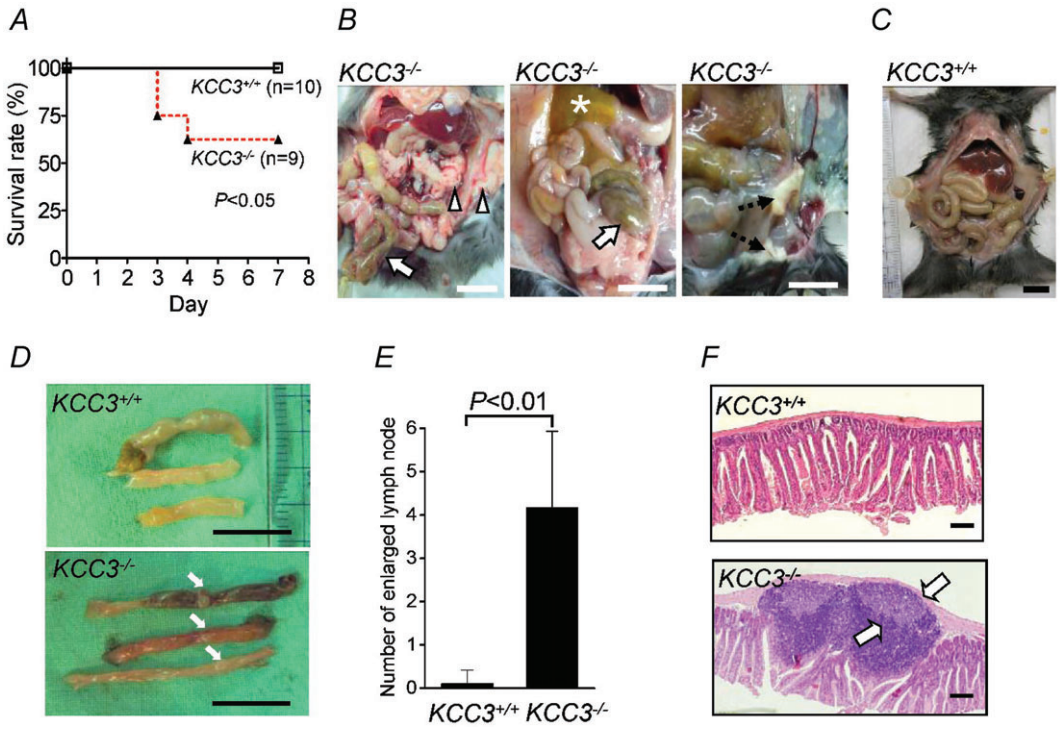

Figure 7. KCC3-deficient mice were more susceptible to infectious challenge
A, Kaplan–Meier curves for $KCC3^{+/+}$ and $KCC3^{-/-}$ mice after intraperitoneal injection with 2.36×10^8 CFU *S. aureus*. *B* and *C*, on the 7th day, all surviving mice were killed and their gastrointestinal tracts were examined. $KCC3^{-/-}$ mice showed distended intestines with stool impaction (arrows), hyperaemic peritoneum (arrowheads), pus formation (star), and caseation (dashed arrows), which were rarely observed in $KCC3^{+/+}$ mice. Scale bar: 1 cm. *D*, unlike the bowel of the $KCC3^{+/+}$ strain (upper panel), that of the $KCC3^{-/-}$ strain showed an increased number of enlarged lymph nodes (lower panel, arrows). Scale bar: 1 cm. *E*, determination of the number of enlarged intestinal lymph nodes. Each bar represented the mean ± SEM ($n = 9$ and 10 for $KCC3^{-/-}$ and $KCC3^{+/+}$ mice, respectively). *F*, haematoxylin–eosin stained sections of the same part of the intestine showed prominent germinal centres (arrows) with abundant internal apoptotic bodies in $KCC3^{-/-}$ mice (lower panel) but not in $KCC3^{+/+}$ mice (upper panel). Scale bar: 200 μm.

Discussion

This study addresses the role of the cation–chloride cotransporter in innate immunity and shows that KCC is necessary for the optimal activation of neutrophils. This conclusion is supported by the following evidence. First, KCC activity is increased simultaneously with the neutrophil activation. Second, KCC activity, but not NKCC activity, is required for the phosphorylation and translocation of phox units as well as the subsequent ROS generation. Third, knockdown of KCC3 (in contrast to that of KCC1 or KCC4) reduces NADPH oxidase activity by altering membrane recruitment and phosphorylation of phox units. Fourth, *KCC3*$^{-/-}$ mice manifest the insufficient NADPH oxidase activity and are more susceptible to bacterial challenge. The increase in white blood cell counts and the change of neutrophil/lymphocyte ratio may be a compensation for dysfunctional *KCC3*$^{-/-}$ neutrophils. This study was approached from various neutrophils of different sources and KCC was blocked by inhibitor, RNAi or knockout. The results support the hypothesis that the KCC family, at least KCC3, contribute to the bactericidal activity of neutrophils. KCC3 knockout mice have been studied for different forms of pathology, such as developing nervous systems and cell volume regulation (Delpire & Mount, 2002; Howard *et al.* 2002; Sun *et al.* 2010). This study is the first one to demonstrate the impaired immunity of KCC3 knockouts.

We explored the mechanisms by which KCC mediates ROS production in activated neutrophils and found that KCC regulates NADPH oxidase activity by altering the phosphorylation and membrane recruitment of phox units. These results were shown on human or murine PMNs treated with the inhibitor, RNAi, or in mice with a genetic knockout. KCC performs two major cellular functions: one is to execute regulatory volume decrease, the other to change cell shape by organizing cytoskeletal dynamics (Delpire & Mount, 2002; Song *et al.* 2002; Shen *et al.* 2003). Neutrophils were swollen by about 23% of their initial volume upon treatment with chemotactic factors (Grinstein *et al.* 1986). NADPH oxidase was also found to be volume sensitive under several circumstances (Friis *et al.* 2008). We have performed the experiments in which neutrophils were swollen before measuring oxidase activity (Fig. S7). Compared with the control groups of neutrophils without swelling, different hypotonic stresses mildly to moderately impaired the NADPH oxidase activation. This implies that the volume regulation is functionally linked with the bactericidal ability of neutrophils. Besides, DIOA through inhibiting KCl activity would inhibit the volume regulation of neutrophils in response to chemotactic factors. As swelling inhibits NADPH oxidase activity, part of the effect of

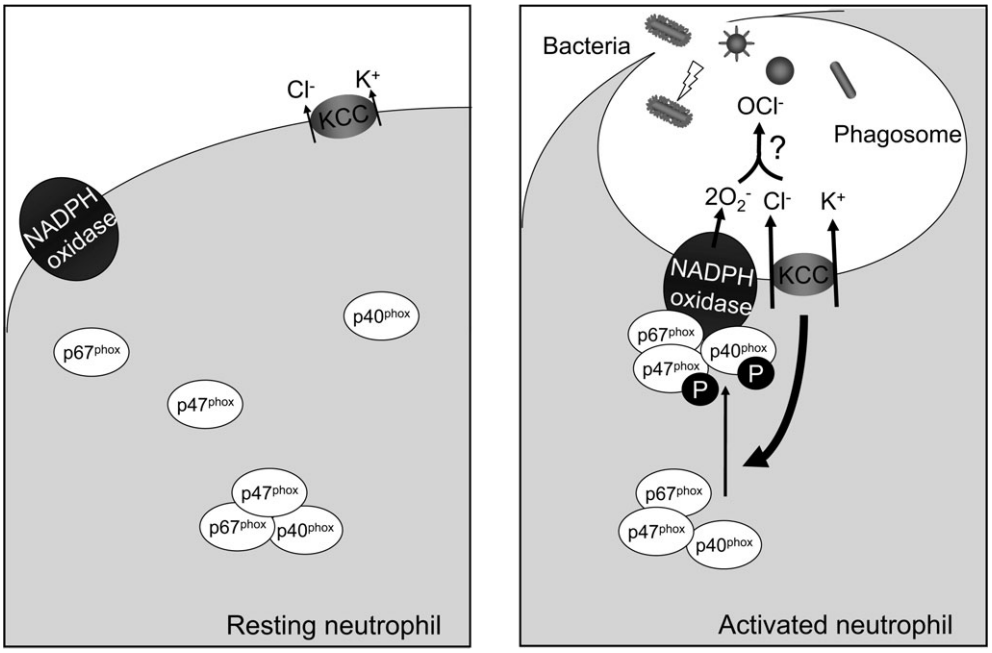

Figure 8. A working model for KCC in the regulation of bactericidal activity
In the resting status of neutrophil, KCC (at least KCC3) and the membrane components of NADPH oxidase are diffusely expressed. In activated neutrophil, NADPH oxidase complexes are associated with KCC3 at the plasma membrane and are internalized to form phagosomes, where KCC activity and expression level affect the production of oxidants. The KCC family might be one of the Cl^- permeation pathways providing the substrate for the generation of OCl^- in phagosomes.

DIOA on NADPH oxidase activity could be through the inhibition of volume regulation.

This study shows that the KCC family affect the cellular events involved in the phox assembly of NADPH oxidase activation. This is likely to be due to the existence of direct or indirect interactions between the KCC family (at least KCC3 isoform), phox units and actin in activated neutrophils. The image results from staining with KCC3, phox units, actin and endosomes imply that these molecules can form a complex during neutrophil activation. Actin is the major network used by cytosolic $p47^{phox}$ or $p40^{phox}$ to position phagosomal protein kinase C, so that phox components can be phosphorylated (Rotrosen & Leto, 1990; Shao *et al.* 2010). Actin also interacts with $p40^{phox}$, primes its binding to phosphatidylinositol 3-phosphate generated during phagosome maturation, and stabilizes the ternary complex at the phagosomal membrane in mature phagosomes (Bissonnette *et al.* 2008). In addition, KCC can organize actin dynamics during regulatory volume decrease (Adragna *et al.* 2004) and probably change the cell shape for engulfment of microbes.

Several Cl^- permeation pathways have been identified in activated neutrophils, including ClC3 channel, CFTR and swelling-activated chloride channel. In contrast, no K^+ permeation pathway has been shown in activated neutrophils. Compared to K^+ flux, there is a bigger Cl^- flux in activated neutrophils (Fig. 1). DIOA, the KCC inhibitor, almost abolished the chemical- or toxin-induced K^+ flux, whereas it inhibited 50–60% of chemical- or toxin-induced Cl^- flux. These results can be explained as follows: (1) there are multiple Cl^- permeation pathways in activated neutrophils and KCC is only one of them; and (2) KCC is likely to be the predominant K^+ permeation pathway in activated neutrophils.

Taking the evidence together, the working model of this study could be proposed as follows (summarized in Fig. 8). KCC (at least KCC3) and the membrane components of NADPH oxidase are diffusely expressed in the resting state of the neutrophil. In activated neutrophil, NADPH oxidase complex is associated with KCC at the plasma membrane and they are internalized to form phagosomes, where KCC activity and expression level affect the production of oxidants. The KCC family might be one of the Cl^- permeation pathways providing the substrate for the generation of OCl^- in phagosomes. However, the current evidence cannot answer whether Cl^- flux into phagosome is required to generate OCl^-. This study supports the notion that KCC, in particular KCC3, is involved in the early stages of the host's defence against microorganisms, which adds to our understanding of the physiological relevance of the KCC family.

References

Adragna NC, Di Fulvio M & Lauf PK (2004). Regulation of K-Cl cotransport: from function to genes. *J Membr Biol* **201**, 109–137.

Allegra M, Furtmuller PG, Regelsberger G, Turco-Liveri ML, Tesoriere L, Perretti M, Livrea MA & Obinger, C (2001). Mechanism of reaction of melatonin with human myeloperoxidase. *Biochem Biophys Res Commun* **282**, 380–386.

Bissonnette SA, Glazier CM, Stewart MQ, Brown GE, Ellson CD & Yaffe MB (2008). Phosphatidylinositol 3-phosphate-dependent and -independent functions of p40phox in activation of the neutrophil NADPH oxidase. *J Biol Chem* **283**, 2108–2119.

Bonvillain RW, Painter RG, Adams DE, Viswanathan A, Lanson NA Jr & Wang G (2010). RNA interference against CFTR affects HL60-derived neutrophil microbicidal function. *Free Radic Biol Med* **49**, 1872–1880.

Busetto S, Trevisan E, Decleva E, Dri P & Menegazzi R (2007). Chloride movements in human neutrophils during phagocytosis: characterization and relationship to granule release. *J Immunol* **179**, 4110–4124.

Delpire E & Mount DB (2002). Human and murine phenotypes associated with defects in cation-chloride cotransport. *Annu Rev Physiol* **64**, 803–843.

El-Benna J, Dang PM, Gougerot-Pocidalo MA, Marie JC & Braut-Boucher F (2009). p47phox, the phagocyte NADPH oxidase/NOX2 organizer: structure, phosphorylation and implication in diseases. *Exp Mol Med* **41**, 217–225.

English D & Andersen BR (1974). Single-step separation of red blood cells. Granulocytes and mononuclear leukocytes on discontinuous density gradients of Ficoll-Hypaque. *J Immunol Methods* **5**, 249–252.

Friis MB, Vorum KG & Lambert IH (2008). Volume-sensitive NADPH oxidase activity and taurine efflux in NIH3T3 mouse fibroblasts. *Am J Physiol Cell Physiol* **294**, C1552–1565.

Fuchs A, Bouin AP, Rabilloud T & Vignais PV (1997). The 40-kDa component of the phagocyte NADPH oxidase (p40phox) is phosphorylated during activation in differentiated HL60 cells. *Eur J Biochem* **249**, 531–539.

Garay RP, Nazaret C, Hannaert PA & Cragoe EC (1988). Demonstration of a [K^+,Cl^-]-cotransport system in human red cells by its sensitivity to [(dihydroindenyl)oxy]alkanoic acids: regulation of cell swelling and distinction from the bumetanide-sensitive [Na^+,K^+,Cl^-]-cotransport system. *Mol Pharmacol* **33**, 696–701.

Graves AR, Curran PK, Smith CL & Mindell JA (2008). The Cl^-/H^+ antiporter ClC-7 is the primary chloride permeation pathway in lysosomes. *Nature* **453**, 788–792.

Grinstein S, Furuya W & Cragoe EJ Jr (1986). Volume changes in activated human neutrophils: the role of Na^+/H^+ exchange. *J Cell Physiol* **128**, 33–40.

Howard HC, Mount DB, Rochefort D, Byun N, Dupre N, Lu J, Fan X, Song L, Riviere JB, Prevost C, *et al.* (2002). The K-Cl cotransporter KCC3 is mutant in a severe peripheral neuropathy associated with agenesis of the corpus callosum. *Nat Genet* **32**, 384–392.

Ince C, Thio B, van Duijn B, van Dissel JT, Ypey DL & Leijh PC (1987). Intracellular K^+, Na^+ and Cl^- concentrations and membrane potential in human monocytes. *Biochim Biophys Acta* **905**, 195–204.

Liu WT, Lin CH, Hsiao M & Gean PW (2011). Minocycline inhibits the growth of glioma by inducing autophagy. *Autophagy* **7**, 166–175.

Matsuda JJ, Filali MS, Moreland JG, Miller FJ & Lamb FS (2010). Activation of swelling-activated chloride current by tumor necrosis factor-α requires ClC-3-dependent endosomal reactive oxygen production. *J Biol Chem* **285**, 22864–22873.

Menegazzi R, Busetto S, Cramer R, Dri P & Patriarca P (2000). Role of intracellular chloride in the reversible activation of neutrophil β2 integrins: a lesson from TNF stimulation. *J Immunol* **165**, 4606–4614.

Menegazzi R, Busetto S, Decleva E, Cramer R, Dri P & Patriarca P (1999). Triggering of chloride ion efflux from human neutrophils as a novel function of leukocyte β2 integrins: relationship with spreading and activation of the respiratory burst. *J Immunol* **162**, 423–434.

Menegazzi R, Busetto S, Dri P, Cramer R & Patriarca P (1996). Chloride ion efflux regulates adherence, spreading, and respiratory burst of neutrophils stimulated by tumor necrosis factor-α (TNF) on biologic surfaces. *J Cell Biol* **135**, 511–522.

Moreland JG, Davis AP, Bailey G, Nauseef WM & Lamb FS (2006). Anion channels, including ClC-3, are required for normal neutrophil oxidative function, phagocytosis, and transendothelial migration. *J Biol Chem* **281**, 12277–12288.

Moreland JG, Davis AP, Matsuda JJ, Hook JS, Bailey G, Nauseef WM & Lamb FS (2007). Endotoxin priming of neutrophils requires NADPH oxidase-generated oxidants and is regulated by the anion transporter ClC-3. *J Biol Chem* **282**, 33958–33967.

Painter RG, Bonvillain RW, Valentine VG, Lombard GA, LaPlace SG, Nauseef WM & Wang G (2008). The role of chloride anion and CFTR in killing of *Pseudomonas aeruginosa* by normal and CF neutrophils. *J Leukoc Biol* **83**, 1345–1353.

Rotrosen D & Leto TL (1990). Phosphorylation of neutrophil 47-kDa cytosolic oxidase factor. Translocation to membrane is associated with distinct phosphorylation events. *J Biol Chem* **265**, 19910–19915.

Rust MB, Alper SL, Rudhard Y, Shmukler BE, Vicente R, Brugnara C, Trudel M, Jentsch TJ & Hubner CA (2007). Disruption of erythroid K-Cl cotransporters alters erythrocyte volume and partially rescues erythrocyte dehydration in SAD mice. *J Clin Invest* **117**, 1708–1717.

Salmon MD & Ahluwalia J (2009). Swell activated chloride channel function in human neutrophils. *Biochem Biophys Res Commun* **381**, 462–465.

Shao D, Segal AW & Dekker LV (2010). Subcellular localisation of the p40phox component of NADPH oxidase involves direct interactions between the Phox homology domain and F-actin. *Int J Biochem Cell Biol* **42**, 1736–1743.

Shen MR, Chou CY, Browning JA, Wilkins RJ & Ellory JC (2001*a*). Human cervical cancer cells use Ca^{2+} signalling, protein tyrosine phosphorylation and MAP kinase in regulatory volume decrease. *J Physiol* **537**, 347–362.

Shen MR, Chou CY, Hsu KF, Liu HS, Dunham PB, Holtzman EJ & Ellory JC (2001*b*). The KCl cotransporter isoform KCC3 can play an important role in cell growth regulation. *Proc Natl Acad Sci U S A* **98**, 14714–14719.

Shen MR, Chou CY, Hsu KF, Hsu YM, Chiu WT, Tang MJ, Alper SL & Ellory JC (2003). KCl cotransport is an important modulator of human cervical cancer growth and invasion. *J Biol Chem* **278**, 39941–39950.

Simchowitz L & De Weer P (1986). Chloride movements in human neutrophils. Diffusion, exchange, and active transport. *J Gen Physiol* **88**, 167–194.

Song L, Mercado A, Vazquez N, Xie Q, Desai R, George AL Jr, Gamba G & Mount DB (2002). Molecular, functional, and genomic characterization of human KCC2, the neuronal K-Cl cotransporter. *Brain Res Mol Brain Res* **103**, 91–105.

Sun YT, Lin TS, Tzeng SF, Delpire E & Shen MR (2010). Deficiency of electroneutral K^+-Cl^- cotransporter 3 causes a disruption in impulse propagation along peripheral nerves. *Glia* **58**, 1544–1552.

Author contributions

Y.T.S. performed experiments, analysed results and wrote the manuscript; C.C.S. designed experiments, established methodology and evaluated primary data; E.D. established the genetic knockout animal, and contributed to the editing of the manuscript; M.R.S. designed the study, evaluated primary data, and contributed to the writing of the manuscript.

Acknowledgements

We thank J. H. Liang for his support with regards to isotope and lucigenin experiments and Dr Y. F. Huang for helpful discussions. This work was partly supported by grants from the National Science Council and the National Cheng Kung University Hospital, Taiwan.